

Cross sections for fusion-like residues for the $^{16}\text{O} + ^{27}\text{Al}$ system up to 25 MeV/nucleon

A. DACAL, M.E. ORTIZ, E. CHÁVEZ-LOMELÍ

*Instituto de Física, Universidad Nacional Autónoma de México
Apartado postal 20-364, Del. A. Obregón. México D.F., México*

J. GÓMEZ DEL CAMPO AND D. SHAPIRA

Oak Ridge National Laboratory, Oak Ridge TN 37831, U.S.A.

Recibido el 6 de octubre de 1994; aceptado el 10 de noviembre de 1994

ABSTRACT. Cross sections for fragments with $3 \leq Z \leq 16$ were measured for ^{16}O bombarding energies of 295 MeV and 400 MeV on ^{27}Al . Results are presented for the measurement corresponding to $Z > 7$. Analysis of the residue-like cross section reveal a 20% of incomplete fusion contribution and a decrease of the cross section with increasing energy, consistent with critical angular momentum limitations. The predicted disappearance of the residue cross section at high energies is not observed.

RESUMEN. Se midieron secciones transversales de fragmentos con $3 \leq Z \leq 16$ para energías de bombardeo de ^{16}O de 295 y 400 MeV sobre blancos de ^{27}Al . Se presentan resultados de las medidas correspondientes a $Z > 7$. El análisis de las secciones de los residuos de evaporación indica que la contribución de fusión incompleta es de 20% y que el decremento de la sección transversal, al aumentar la energía, es consistente con limitaciones impuestas por el momento angular crítico. La desaparición de la sección de residuos de evaporación para alta energía no se observa.

PACS: 25.70.-z; 25.70.Gh; 25.70.Pq

1. INTRODUCTION

The disappearance of fusion-like residue cross sections as the bombarding energy increases is a subject of current interest [1,2], mainly because the predicted energy for which this disappearance should occur is sensitive to the choice of in medium nucleon-nucleon interaction in the nuclear matter equation of state [1]. Some indication of the vanishing of the evaporation residue-like component have been given experimentally in the $^{40}\text{Ar} + ^{27}\text{Al}$ system, studied between 20 and 40 MeV/nucleon [3], by analysing the shape of the energy spectra. Also the $^{40}\text{Ar} + ^{68}\text{Zn}$ system at energies up to 35 MeV/nucleon [4] shows a steady decrease of the fusion-like cross section as a function of energy. To date no other studies exist that address this topic in medium mass composite nuclei. For lighter systems the $^{14}\text{N} + ^{10}\text{B}$ reaction has been reported recently [5] up to 18 MeV/nucleon, and although the fusion-like cross section continues to decrease with increasing energy it is still consistent with critical angular momentum limitations.

The $^{16}\text{O} + ^{27}\text{Al}$ system has been studied at low energies by several authors [6,7] and also up to 19 MeV/nucleon [8,9,10]. The cross section for fusion-like residues were extracted

by velocity centroids [8] and by detailed analysis of the shape of velocity spectra [9]. In both works, contributions up to 20% of incomplete fusion (IF) were deduced. Additional studies [10] of particle-particle correlations up to 215 MeV bombarding energy reveal reaction decay times consistent with complete fusion. In all these previous experiments the bombarding energies used are too low to be significant for the study of the disappearance of the fusion-like cross section. In the present work the measurement of residue-like cross sections for the $^{16}\text{O} + ^{27}\text{Al}$ system have been extended to higher energies: 18.4 and 25 MeV/nucleon. The main difficulty with measurements at high energies, such as the ones reported here, is the identification of the residue-like component. Due to the high excitation energy reached in the compound nucleus, the evaporated mass can be close to that of the target or the projectile, producing a residue whose charge can overlap with either that of the target or the projectile. One way to deal with this difficulty consist of analyzing the energy or velocity spectra to determine whether full momentum transfer or IF has been achieved. In the following sections the data will be presented and compared with detailed statistical model calculations made with the code LILITA [11].

2. EXPERIMENTAL TECHNIQUES

Reaction products with $3 \leq Z \leq 16$, arising from collisions of ^{16}O on an ^{27}Al target were measured using ^{16}O beams of 295 MeV and 400 MeV extracted from coupled operation of the tandem and cyclotron of the Holifield Heavy Ion Research Facility (HHIRF). Large ionization chamber-solid state detector systems were used to register the fragments for $5^\circ \leq \theta_{\text{lab}} \leq 20^\circ$. One detector system consisted of a large ionization chamber used as ΔE stage and two position sensitive solid state detectors used as E . This system covered an interval of laboratory scattering angles of 10° . The rest of the detectors were conventional telescopes $E - \Delta E$ solid state systems placed at very forward angles $5^\circ \leq \theta_{\text{lab}} \leq 10^\circ$. Unit Z resolution was achieved for $3 \leq Z \leq 16$. The ^{27}Al target consisted of a foil 6.25 μm thick, equivalent to an areal density of 1.7 mg/cm^2 . Absolute cross sections were determined by beam current integration and Rutherford scattering.

Energy spectra of fragments lighter than $Z = 8$ show typical beam energy components characteristic of projectile-like fragments, and therefore will not be discussed. Typical spectra of products of $Z = 10$ and $Z = 12$ are shown in Figs. 1 and 2. Figure 1 shows the spectra taken at a beam energy of 295 MeV for Ne fragments (bottom) and for Mg fragments (top) at a laboratory angle of 12° . For the Ne case, two components are clearly seen: one at $\langle E \rangle = 250$ MeV direct reaction-like and the other at $\langle E \rangle = 50$ MeV which is characteristic of complete-incomplete fusion mechanisms (central collisions). Figure 2 shows the spectra for Ne and Mg fragments at a bombarding energy of 400 MeV and a laboratory scattering angle of 12° . In this spectrum a single component is clearly dominant. For the case of Mg (top) at an energy $\langle E \rangle = 75$ MeV, characteristic of central collisions. The case of the Ne residues (bottom) is similar to the one at 295 MeV. The solid lines in Figs. 1 and 2 are the results of statistical model calculations and will be discussed in the next section.

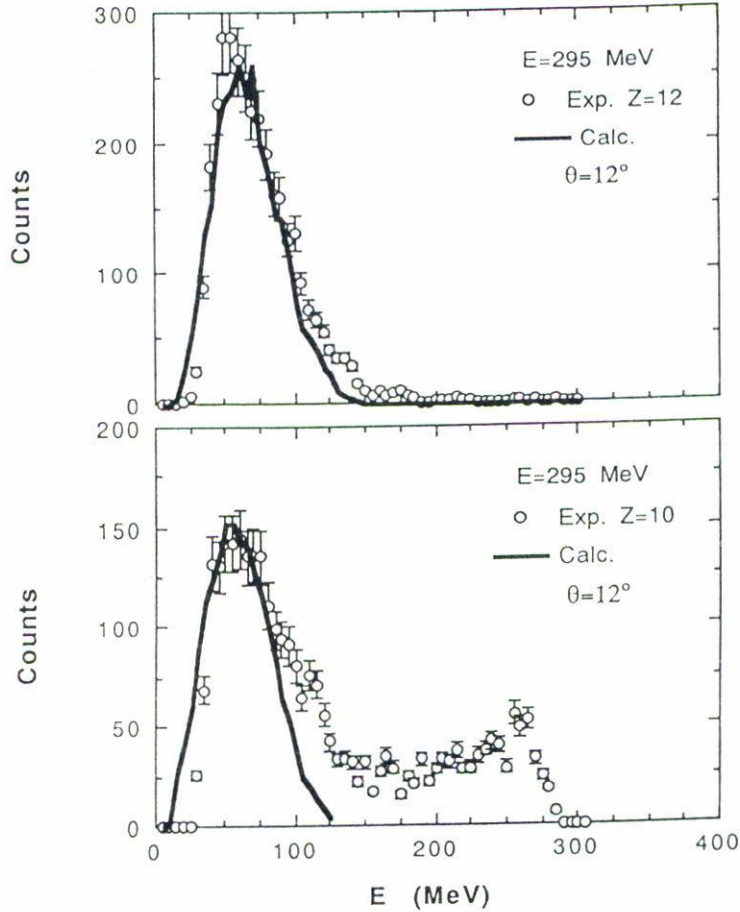


FIGURE 1. Experimental energy spectrum (open circles) for Ne residues (bottom) and for Mg (top) of the $^{16}\text{O} + ^{27}\text{Al}$ reaction at $E(^{16}\text{O}) = 295$ MeV. The solid line is the calculated spectrum using the Monte Carlo code LILITA discussed in the text.

3. ANALYSIS

In order to obtain the residue-like angle-integrated cross sections it is important first to analyze in detail the energy spectra of the fragments such as those given in Figs. 1 and 2. Previous measurements of the $^{16}\text{O} + ^{27}\text{Al}$ system [8,9] reported IF contributions as high as 26% of the total residue-like cross sections. Even at ^{16}O energies as low as 150 MeV [7] IF of 20% was reported. For the calculations of the energy spectra in the present study a 20% contribution of IF has been chosen, since this is the value predicted by the systematics [12] at 295 MeV bombarding energy. Consistent with Refs. [7] and [12] only α particles lost from the projectile have been considered as IF channels. The inclusion of other IF channels like p and n differ very little from the prediction of complete fusion and therefore were not included in the simulations. The calculations were done with the code LILITA [11], which uses the Hauser-Feshbach formula in a Monte Carlo approach. A set of statistical model parameters which fit measurements at lower energies for systems of similar masses [6,9,13]

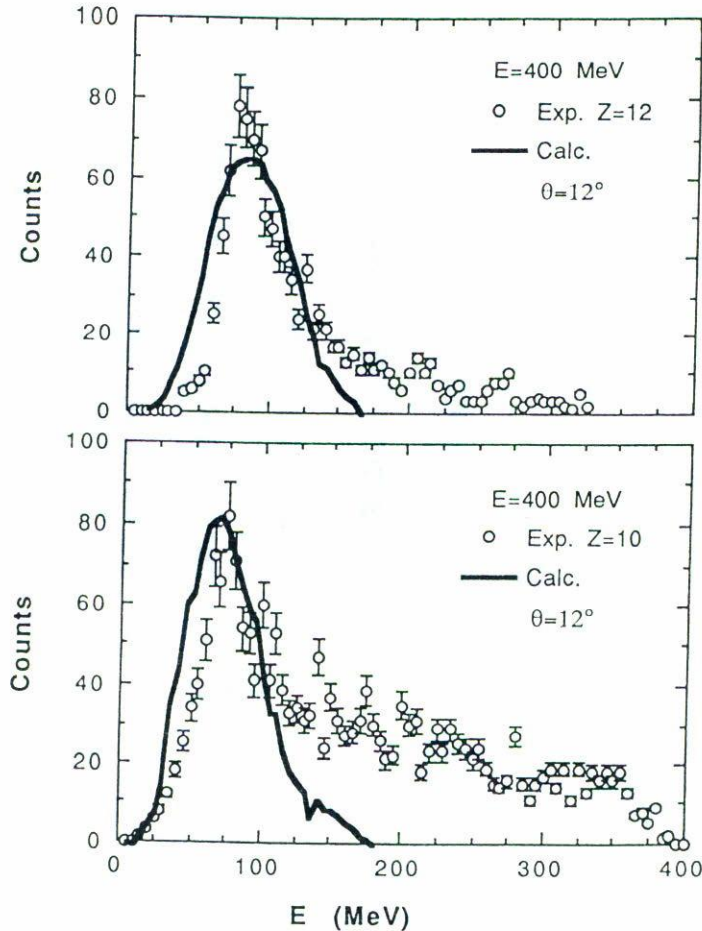


FIGURE 2. Experimental energy spectrum (open circles) for Ne residues (bottom) and for Mg (top) of the $^{16}\text{O} + ^{27}\text{Al}$ reaction at $E(^{16}\text{O}) = 400$ MeV. The solid line is the calculated spectrum using the Monte Carlo code LILITA.

were used. For the complete fusion part, the calculations were done using a critical angular momentum value of $32 \hbar$, as suggested in Ref. [14], reducing however the absolute value of the fusion cross section by 20%. For the IF channel, the value of $26 \hbar$ was used (this value extracted from Ref. [14] corresponds to the $^{12}\text{C} + ^{27}\text{Al}$ fusion).

The results of the calculations are shown in the solid lines in Figs. 1 and 2. In Fig. 1, the calculations are done for 295 MeV bombarding energy and for $Z = 10$ and $Z = 12$ fragments. The calculation was normalized to the data for better shape comparison. From the comparisons shown in Fig. 1, it can be seen that the lower energy component (50 MeV) agrees reasonable well with the expected spectrum for central collisions. If heavier IF channels (like Li or Be) were to be included in the fusion spectra, the agreement with experimental data would not be as good, since this channels shift the maxima of the calculated spectra to lower energies. For the higher energy, at 400 MeV, the calculation is shown in Fig. 2 also for $Z = 10$ and $Z = 12$ fragments and again compares well to the experimental spectrum. This calculation was performed also with 20% contribution

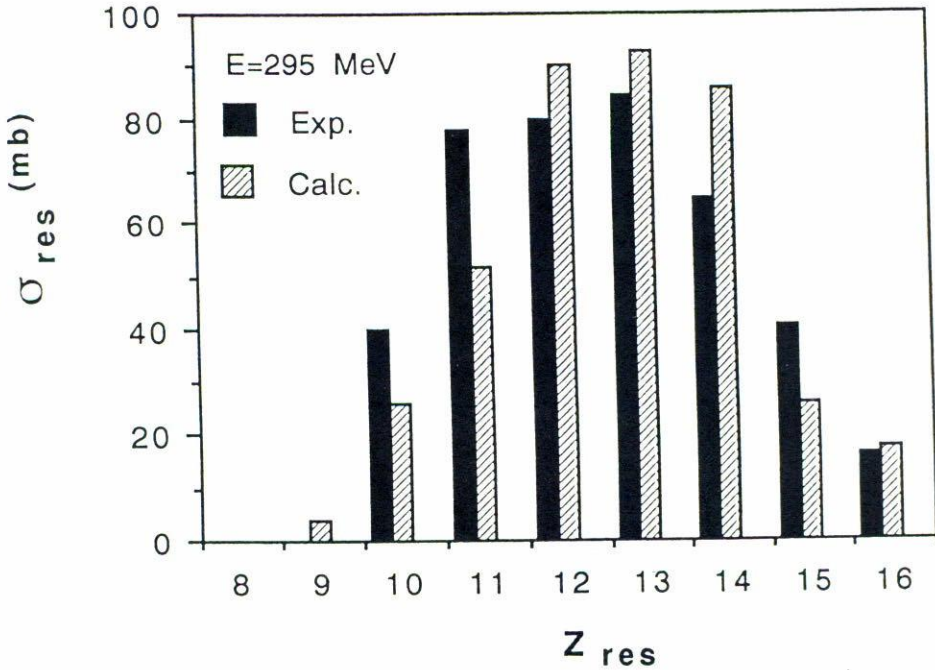


FIGURE 3. Angle integrated yield (in mb) of the fusion-like component (low energy group of figure 1) plotted as a function of Z . The solid histogram is for the experimental data and the open histogram the Monte Carlo calculation. The bombarding energy is 295 MeV.

for the IF component, even though for this higher energy a slightly higher value (25%) should be expected according to the systematics [12]. Our analysis will not be sensitive to such small changes on the IF contributions. The main point to be drawn from the comparisons in Figs. 1 and 2 is that the region of central collisions can be identified using the calculated spectra as a guide, so the experimental cross section for residue-like events can be extracted at each angle.

The residue-like cross sections (σ_{res}) obtained are shown in Figs. 3 and 4 as a function of Z_{res} . The solid histograms correspond to the experimental values and the open histograms to the calculated ones. As can be seen in Fig. 3, the experimental Z distribution is reproduced rather well by the calculation. It is also important to note that the average residue Z is about 13 which is 8 charge units removed from the compound nucleus. For the higher energy of 400 MeV, the comparisons shown in Fig. 4 are not as good as that for 295 MeV, but they follow the same general trend. One point of concern for the highest energies is the large amount of residue cross section found for $Z = 8$ (68 mb) compared to 40 mb predicted by the calculation since for this Z there is strong contamination of beam scattering at very forward angles. At this high bombarding energy, the compound nucleus is formed at 265 MeV excitation energy. A region where suitable values for the parameters involved in a statistical model calculation are not well known.

The absolute total cross sections (in mb) for the residues (σ_{res}), summed over Z , are given by the solid dots in Fig. 5. The cross section at 295 MeV was 402 ± 40 mb and for 400 MeV it was 270 ± 30 mb. The open dots correspond to previous measurements [15–

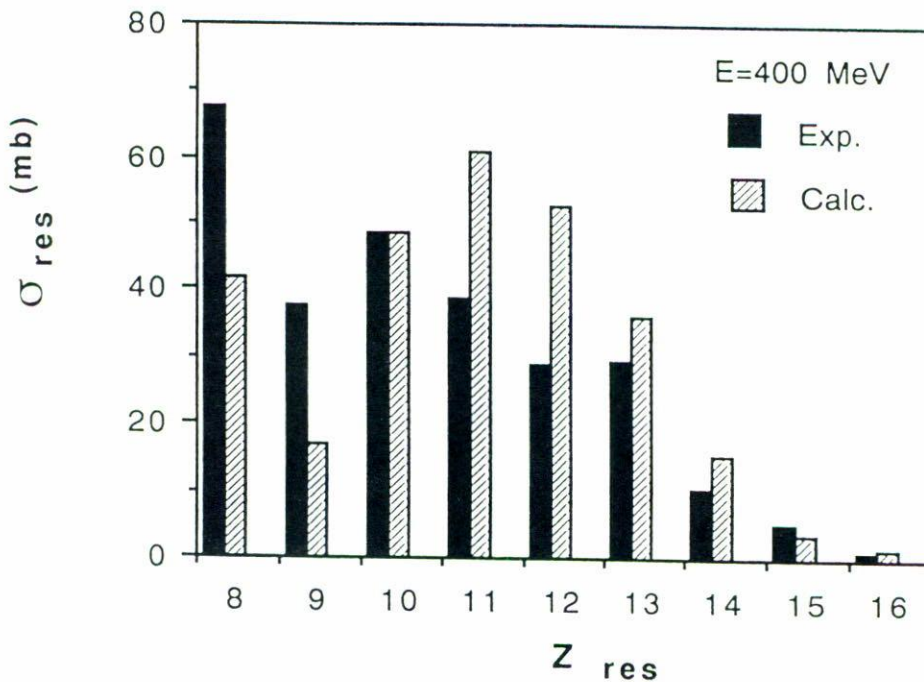


FIGURE 4. Angle integrated yield (in mb) of the fusion-like component (low energy group of figure 2) plotted as a function of Z . The solid histogram is for the experimental data and the open histogram the Monte Carlo calculation. The bombarding energy is 400 MeV.

20] of mostly complete fusion, except for the point at 215 MeV (13.4 MeV/nucleon) which corresponds to the measurements of Ref. [6], which includes approximately 20% contribution of IF. The solid curve in Fig. 5 corresponds to the calculation of reference [14] for only the complete fusion cross section and a critical angular momentum of $32\hbar$.

A full interpretation of the data given in Fig. 5 is difficult because above 10 MeV/nucleon IF sets in and a clean extraction of the fusion cross section is no longer possible. However a generalization of fusion to central collisions (or fusion-like) defined by the sum of the complete and incomplete fusion components is useful, as was shown in Ref. [1]. The fact that the data follows the complete fusion calculation indicates that the critical angular momentum limitation is still the important factor. Certainly will be of value to perform Boltzmann-Uehling-Uhlenbeck equation (BUU) calculations like those done [1] for the $^{40}\text{Ar} + ^{27}\text{Al}$ and $^{40}\text{Ca} + ^{40}\text{Ca}$ systems for which the threshold for disappearance of fusion-like cross sections occurs around 30–40 MeV/nucleon, depending on the choice of a nucleon-nucleon interaction in the nuclear matter equation of state. For the $^{16}\text{O} + ^{27}\text{Al}$ system, the experimental evidence is that this threshold, if present, should be well above 25 MeV/nucleon.

ACKNOWLEDGEMENTS

Oak Ridge National Laboratory is managed by Martin Marietta Energy Systems, Inc.

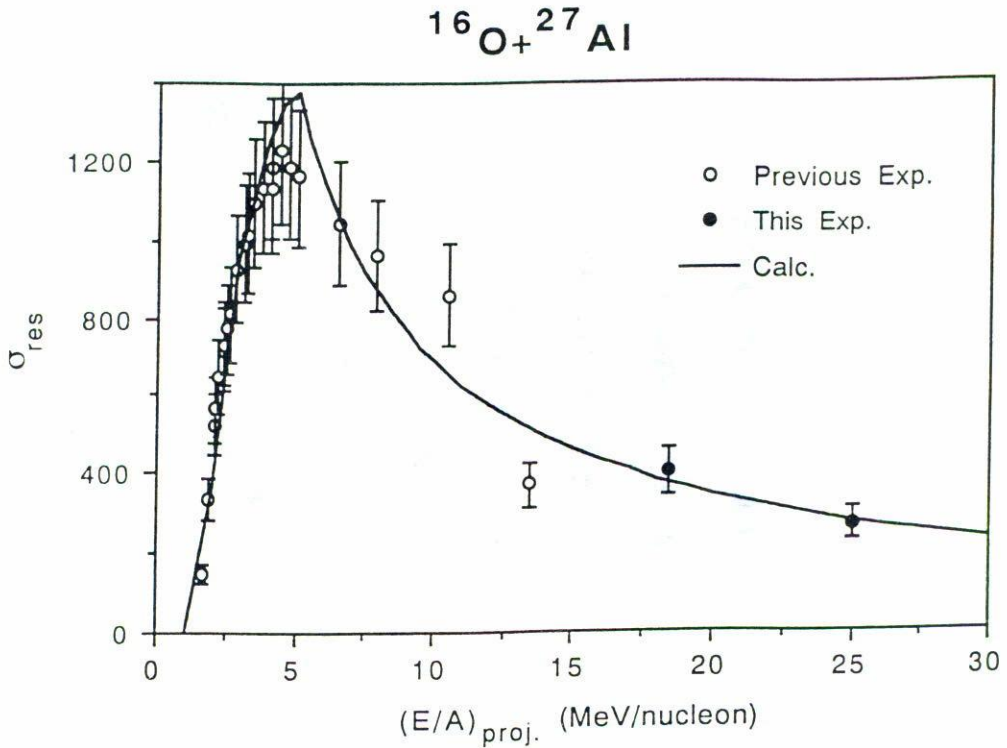


FIGURE 5. Residue cross section in mb (defined as the sum of complete and incomplete fusion) as a function of the bombarding energy in MeV/nucleon. The open dots are the measurements of references [9], [15–20] and the solid dots are the present measurements. The solid curve is the prediction of the fusion cross section given in Ref. [14].

under contract DE-AC05-84OR21400 with the U.S. Department of Energy. Three of us (AD, MEO and EC) want to acknowledge partial support from CONACYT (Mexico) under contract number 1103-E9102.

REFERENCES

1. H.M. Xu, W.G. Lynch, P. Danielewicz, and G.F. Bertsch, *Phys. Rev. Lett.* **65** (1990) 843.
2. H.M. Xu, *Phys. Rev.* **C46** (1992) R389.
3. G. Auger, E. Plagnol, D. Jouan, C. Guet, D. Heurer, M. Maurel, H. Nifenecker, C. Ristori, F. Schussler, H. Doubre, and C. Gregoire, *Phys. Lett.* **169B** (1986) 161.
4. A. Fahli, J.P. Coffin, G. Guillaume, B. Heusch, F. Jundt, F. Rami, A.J. Cole, S. Kox, and Y. Schutz, *Phys. Rev.* **C34** (1986) 161.
5. M.E. Ortiz, E.R. Chávez, A. Dacal, J. Gómez del Campo, Y.D. Chan, and R. G. Stokstad, *Rev. Mex. Fís.* **38** (1992) 543.
6. H. Ikezoe, N. Shikazono, Y. Tomita, Y. Sugiyama, and K. Ideno, *Nucl. Phys.* **A444** (1985) 349.
7. H. Ikezoe, N. Shikazono, Y. Tomita, K. Ideno, and Y. Sugiyama, *Nucl. Phys.* **A462** (1987) 150.
8. Y. Chang, M. Murphy, R.G. Stokstad, I. Tseruya, and S. Wald, *Phys. Rev.* **C27** (1983) 447.

9. G.P. Gilfoyle, M.S. Gordon, R.L. McGrath, G. Auger, J.M. Alexander, D.G. Kovar, M.F. Vineyard, C. Beck, D.J. Henderson, P.A. DeYoung, and D. Kortering, *Phys. Rev.* **C46** (1992) 265.
10. P.A. DeYoung, C.J. Gelderloos, D. Kortering, J. Sarafa, K. Zienert, M.S. Gordon, B.J. Feneman, G.P. Gilfoyle, X. Lu, R.L. McGrath, D.M. de Castro Rizzo, J.M. Alexander, G. Auger, S. Kox, L.C. Vaz, C. Beck, D.J. Henderson, D.G. Kovar, and M.F. Vineyard, *Phys. Rev.* **C41** (1990) 1885.
11. J. Gómez del Campo and R. G. Stokstad, Oak Ridge National Laboratory Technical Memo No. ORNL-TM-7295 (1981).
12. H. Morgenstern, W. Bohne, W. Galster, K. Grabisch, and A. Kyanowski, *Phys. Rev. Lett.* **52** (1984) 1104.
13. S.J. Sanders, D.G. Kovar, B.B. Back, C. Beck, D.J. Henderson, R.V.F. Janssens, T.F. Wang, and B.D. Wilkins, *Phys. Rev.* **C40** (1989) 2091.
14. W.W. Wilke, J.R. Birkelund, H.J. Wollershein, A.D. Noover, J.R. Huizenga, W.V. Shroeder, and L.E. Tubbs, *Atomic and Nuclear Data Tables* **25** (1980) 391.
15. Y. Eisen, I. Tserruya, Y. Eyal, Z. Fraenkel, and M. Hillman, *Nucl. Phys.* **A291** (1977) 459.
16. B. Back, R.R. Betts, C. Gaarde, J.S. Larsen, E. Michelsen, and Tai Kuang-Hsi, *Nucl. Phys.* **A285** (1977) 317.
17. J. Dauk, K.P. Lieb, and A.M. Kleinfeld, *Nucl. Phys.* **A241** (1975) 170.
18. R.L. Kozub, N.H. Lu, J.M. Miller, D. Logan, T.W. Debiak, and L. Kowalski, *Phys. Rev.* **C11** (1975) 1497.
19. R. Rascher, W.F.J. Muller, and K.P. Lieb, *Phys. Rev.* **C20** (1979) 1029.
20. D.G. Kovar, D.F. Geesaman, T.H. Braid, Y. Eisen, W. Henning, T.R. Ophel, M. Paul, K.E. Rehm, S.J. Sanders, P. Sperr, J.P. Schiffer, S.L. Tabor, S. Vigdor, and B. Zeidman, *Phys. Rev.* **C20** (1979) 2170.